REPORT DOCUMENTATION PAGE

Form Approved OMB No. 0704-0188

1. REPORT DATE *(DD-MM-YYYY)*	2. REPORT TYPE	3. DATES COVERED *(From - To)*
	Technical Papers	

4. TITLE AND SUBTITLE

5a. CONTRACT NUMBER

5b. GRANT NUMBER

5c. PROGRAM ELEMENT NUMBER

6. AUTHOR(S)

5d. PROJECT NUMBER 3058

5e. TASK NUMBER RF9A

5f. WORK UNIT NUMBER

7. PERFORMING ORGANIZATION NAME(S) AND ADDRESS(ES)

Air Force Research Laboratory (AFMC)
AFRL/PRS
5 Pollux Drive
Edwards AFB CA 93524-7048

8. PERFORMING ORGANIZATION REPORT

9. SPONSORING / MONITORING AGENCY NAME(S) AND ADDRESS(ES)

Air Force Research Laboratory (AFMC)
AFRL/PRS
5 Pollux Drive
Edwards AFB CA 93524-7048

10. SPONSOR/MONITOR'S ACRONYM(S)

11. SPONSOR/MONITOR'S NUMBER(S)

12. DISTRIBUTION / AVAILABILITY STATEMENT

Approved for public release; distribution unlimited.

13. SUPPLEMENTARY NOTES

14. ABSTRACT

15. SUBJECT TERMS

16. SECURITY CLASSIFICATION OF:			17. LIMITATION OF ABSTRACT	18. NUMBER OF PAGES	19a. NAME OF RESPONSIBLE PERSON
a. REPORT	b. ABSTRACT	c. THIS PAGE			Leilani Richardson
Unclassified	Unclassified	Unclassified	A		19b. TELEPHONE NUMBER *(include area code)* (661) 275-5015

21 separate items enclosed

3058KF9M

MEMORANDUM FOR PR (In-House Publication)

FROM: PROI (TI) (STINFO) 03 May 2000

SUBJECT: Authorization for Release of Technical Information, Control Number: **AFRL-PR-ED-TP-2000-104**
P.A Strakey, D.G. Talley, "Spray Characteristics of Impinging Jet Injectors at High Back-Pressure"

8th International Conference on Liquid Atomization and Spray Systems (Statement A)
(Pasadena, CA, 16-20 Jul 00) (Submission Deadline: 31 May 00)

1. This request has been reviewed by the Foreign Disclosure Office for: a.) appropriateness of distribution statement, b.) military/national critical technology, c.) export controls or distribution restrictions, d.) appropriateness for release to a foreign nation, and e.) technical sensitivity and/or economic sensitivity.
Comments:_____

Signature _____ Date _____

2. This request has been reviewed by the Public Affairs Office for: a.) appropriateness for public release and/or b) possible higher headquarters review.
Comments: _____

Signature _____ Date _____

3. This request has been reviewed by the STINFO for: a.) changes if approved as amended, b.) appropriateness of distribution statement, c.) military/national critical technology, d.) economic sensitivity, e.) parallel review completed if required, and f.) format and completion of meeting clearance form if required
Comments:_____

Signature _____ Date _____

4. This request has been reviewed by PR for: a.) technical accuracy, b.) appropriateness for audience, c.) appropriateness of distribution statement, d.) technical sensitivity and economic sensitivity, e.) military/ national critical technology, and f.) data rights and patentability
Comments:_____

APPROVED/APPROVED AS AMENDED/DISAPPROVED

_____

ROBERT C. CORLEY (Date)
Senior Scientist (Propulsion)
Propulsion Directorate

Eighth International Conference on Liquid Atomization and Spray Systems, Pasadena, CA, USA, July 2000

Spray Characteristics of Impinging Jet Injectors at High Back-Pressure

P. A. Strakey* and D. G. Talley
Air Force Research Laboratory
AFRL/PRSA
10 E. Saturn Blvd. Edwards AFB, CA 93524

Abstract

Atomization characteristics of an impinging jet injector were studied over a range of injection velocities and back-pressures typical of liquid rocket injectors. Sheet breakup length was measured by strobe light imaging and was found to decrease with increasing injection velocity and chamber pressure. The experimentally measured breakup length was compared to linear stability theory and agreement was found to improve with increasing chamber gas density. At low chamber pressures, disturbances due to impact waves were believed to be the primary breakup mechanism. Measurements of droplet size distribution were made with a combination of laser diffraction and droplet imaging instruments. Droplet size was found to be a highly non-linear function of chamber pressure and axial distance from the impingement point. Sauter mean diameter was found to decrease with increasing chamber pressure and axial distance. Secondary atomization was believed to be the breakup mechanism responsible for this dependence. The width of the droplet size distribution was also found to be a function of chamber pressure.

Introduction

A common injector used for both boost and orbit transfer liquid space propulsion is the impinging jet injector. Impinging injectors have been used successfully for many years in a variety of engines (F-1, Titan, H-1), but are often operated at sub-optimum performance in order to maintain adequate chamber wall protection and combustion stability. For high-pressure boost engines and pre-burners, which can operate at pressures on the order of 20 MPa, impinging injectors are typically used in a like-on-like configuration with liquid oxygen and kerosene as propellants. In this configuration, two oxidizer streams are impinged on one another to form a liquid oxidizer sheet. The sheet rapidly breaks up into large ligaments which in turn break up into smaller droplets forming an elliptically shaped spray fan. A fuel spray fan is formed in a similar fashion and the two sprays are overlapped to provide propellant mixing within a single element. Several hundred elements are arranged across the injector faceplate to provide the total propellant flow.

There have been several experimental cold-flow studies that have shown a sensitivity of spray characteristics to injector design and operating conditions [1-5]. Only a few of these studies investigated the effects of chamber pressure, and most of these studies were limited to relatively low chamber pressures (P_c < 2 MPa) relative to typical rocket operating conditions [2-5]. Lower simulation cold-flow pressures are often justified based on a gas density similar to the chemical equilibrium gas density for the higher pressure hot-fire conditions. It is not clear however, that the equilibrium gas density is the appropriate gas density to use in calculating droplet size, especially near the injector faceplate where much of the atomization is taking place.

Lourme [2] and Hautman [3] provided correlations of mass median droplet size with injector operating conditions. Lourme's correlation had a gas density power dependence of -0.2 and a velocity dependence of -0.95. Lourme also showed a decrease in the width of the droplet size distribution with increasing gas density. Hautman provided a similar correlation with a gas density raised to the -0.16 power and velocity raised to the power of 1.24.

Dombrowski and Hooper [4] found that a single correlation could not capture the effects of gas density on mean droplet size. They provided three correlations with a gas density dependence that increased with increasing gas density. Their correlations resulted in gas density raised to the -0.1 to 0.25 power over the range of gas densities from 1.2 to 16.0 kg/m^3.

Anderson *et al.* [5] measured sheet breakup length and droplet size over a range of chamber pressures from 0.1 to 1.05 MPa. The found that breakup length decreased with increasing chamber gas density and that the non-dimensional breakup length, X_b/d_o, could be correlated as a function of Weber number based on the liquid jet properties and the gas to liquid density ratio. They also found a drop size dependency on gas density

* Corresponding author

similar to that of Lourme and Hautman. An impact wave breakup mechanism, similar to that proposed by Dombrowski and Hooper was believed to govern the resulting droplet size.

One of the goals of this investigation is to expand the database of droplet size and sheet breakup length to gas densities up to 118 kg/m^3 (P_c=10.44 MPa). Since spray combustion modeling is of primary interest with respect to this type of data, an increased understanding of the atomization mechanisms of impinging jet injectors is also sought. Ultimately it is hoped that primary and secondary atomization models appropriate for rocket combustor conditions can be developed precluding the use of engineering droplet size correlations which are currently being used as modeling boundary conditions [6].

Experimental Facility

The experimental facility is capable of characterizing full scale single element rocket injectors in cold flow at pressures to 13.8 MPa. Water, which is used as a simulant, is stored and pressurized in a 1 m^3 tank. The injector flow rates are controlled with throttling valves and measured with turbine flow meters to an accuracy of +/- 1%. Chamber pressure is measured to within +/- 0.5% and is pressurized with nitrogen at ambient temperature. The chamber consists of a 0.5 m diameter stainless steel, optically accessible pressure vessel. Three 50 mm and one 120 mm sapphire windows provided optical access to the chamber for spray imaging and for droplet size measurements.

The injector used in this study was a like-on-like impinging injector manufactured by EDM drilling of a stainless steel plate. The orifices were sharp-edged with a diameter of 1.194 mm, L/D ratio of 18.4, impingement angle of 60° and a pre-impingement distance of 5.96 mm. The injector plate was mounted on a manifold with a large plenum to reduce manifold cross-flow effects. The manifold was mounted on a translating stage within the chamber to allow radial and axial movement of the injector with respect to the measurement point.

Measurements were made at injection velocities ranging from 5 to 50 m/s and with chamber pressures of 0.1 to 10.44 MPa. The variation in Reynolds number studied was Re = $6x10^3$ to $6x10^4$ and Weber number based on injector orifice diameter and chamber gas density of We = $4.7x10^{-1}$ to 4.8 x 10^3. Measurements were made at x = 46 mm, 84 mm and 122 mm from the impingement point (Figure 1) along the centerline of the injector axis ($z = y = 0$).

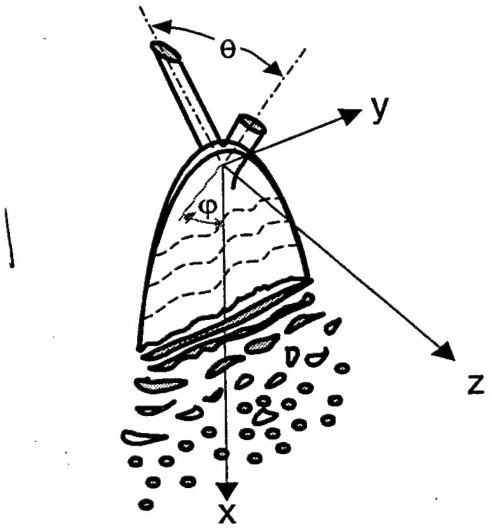

Figure 1: Coordinate system used for measurements.

Spray breakup length was measured using a strobe back-lighting technique. The strobe had a duration of 5 µs and a CCD camera and VCR were used to capture instantaneous images of the spray. The field of view was approximately 60 x 45 mm.

Initial experiments indicated a multitude of diagnostic problems associated with the operating conditions of interest. At low injection velocities (V_j=5 m/s), the maximum observed droplet size was highly non-spherical and on the order of 5000 µm at the lower chamber pressures. A Phase Doppler interferometer (PDI) was initially used to make droplet size measurements. Although the PDI instrument could be optically configured to measure these large sizes, the validity of the measurement with these highly non-spherical droplets was questionable. At the highest injection velocities (V_j=50 m/s) multiple droplet occurrences in the probe volume were observed even at the smallest formable probe volume of 60 µm. It was therefore deemed that PDI measurements at these conditions were not possible. In order to accurately measure the broad range of droplet sizes encountered here, a combination of droplet imaging and laser diffraction instruments was used.

A Greenfield Instruments (model 700) imaging droplet sizer was configured with a long-distance telescopic lens to provide a measurable droplet size range of 40 µm to 7500 µm over a depth of field of about 20 mm. Focus rejection and a depth of field correction were employed to account for the variation in depth of field with droplet size. A Malvern Instruments (model 2600c) laser diffraction droplet sizer was used with a 10 mm beam diameter and a 300

mm range lens to yield a measurable size range of 5.8 μm to 564 μm. The light scattering data was found to best fit the Rosin-Rammler distribution, which was used for all of the data presented here. Also, a multiple scattering correction was employed which allowed measurements to be made at Obscurations ($1-I/I_o$) up to 0.975. The chamber pressurization gas was maintained at ambient temperature and the chamber was pressurized slowly to minimize refractive index gradients within the chamber which were found to cause beam steering problems with the Malvern measurements.

The final droplet size distribution was obtained by "splicing" the two volume distributions together using the droplet size data in the overlapping region to normalize the two distributions. The final measurable droplet size range was 5.8 μm to 7500 μm. Note that the droplet size distribution measured with the Greenfield and Malvern instruments is a line-of-sight spatial size distribution as opposed to a temporal size distribution at a single point in space. Also, both instruments tend to yield diameters based on the average droplet cross-sectional area and are not highly sensitive to droplet shape.

For the higher injection velocities ($V_j \geq 20$ m/s) a flow splitter was employed to reduce the optical attenuation and multiple scattering within the spray. Spray imaging in the absence of the flow splitter indicated a maximum droplet size of about 1500 μm for $V_j = 20$ m/s at all chamber pressures. A splitter plate separation distance of 4.5 mm was chosen to minimize intrusive impact on the spray. Imaging measurements with the flow splitter in place indicated very little effect of the flow splitter on the measured droplet size distribution. The splitter plate does provide some spatial resolution to both the imaging and laser diffraction measurements. At the lower velocities ($V_j <$ 20 m/s), the depth of field of both instruments is greater than the thickness of the spray, which was measured to be less than about 20 mm in the z direction at an axial distance of 122 mm. Therefore, the measured droplet size is an average in the z direction. Traversing the spray in the z direction with the flow splitter in place indicated that there was very little variation in droplet size in the z direction at the lower injection velocities. This is in agreement with the spatially resolved PDI measurements of Hautman [3].

Results and Discussion

Liquid Sheet Breakup

Figure 2 contains a series of spray images spanning the entire range of injection velocity and chamber pressure studied here. Liquid sheet breakup length, as measured from the impingement point to the extent where the intact sheet no longer exists can be seen to generally decrease both with increasing injection

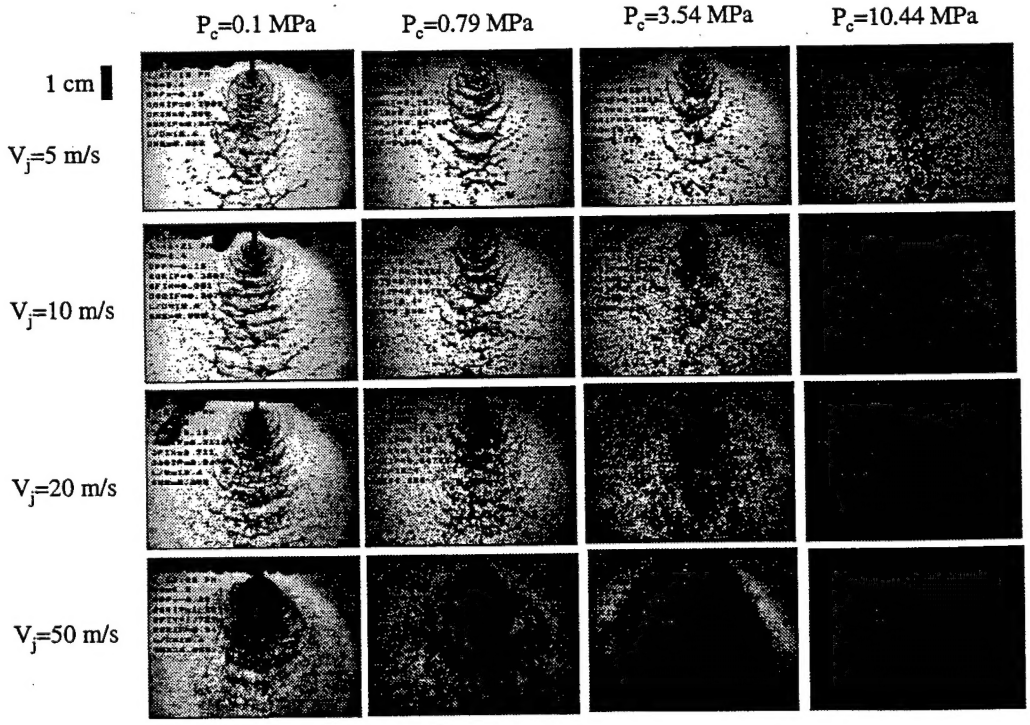

Figure 2: Instantaneous images of spray (viewing in z direction) at 0.1 MPa to 10.44 MPa (left to right) and 5 m/s to 50 m/s (top to bottom). d_o=1.194 mm, L/D=18.4, θ=60°.

velocity and chamber pressure. At a chamber pressure of 10.44 MPa (ρ_g=118 kg/m^3), breakup appears to occur very close to the impingement point.

At each run condition breakup length was measured to be the average of 30 images and is plotted in Figure 3 in non-dimensional form for several injection velocities. Due to the high optical attenuation at the higher injection velocities and chamber pressures, breakup length could only be measured up to V_j=20 m/s. At atmospheric pressure (P_c=0.1 MPa) breakup length increased as jet velocity was increased from 5 m/s to 10 m/s, but significantly decreased as jet velocity was further increased. Anderson *et al.* [7] and Heidmann *et al.* [8] have observed an increase in breakup length for jet velocities up to 18 m/s for long (L/D > 80) orifices at atmospheric back pressure. The decrease in breakup length for velocities greater than 10 m/s observed here could be due to the shorter L/D of 18.4 used in this study. A higher turbulence intensity just prior the point of impingement would be expected with a shorter L/D orifice since most of the turbulence is generated near the orifice inlet and would have less time to decay to a fully developed condition. The higher turbulence intensity would be expected to contribute to increased impact wave disturbances in the liquid sheet.

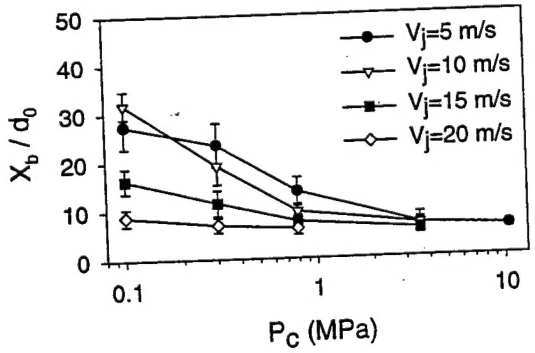

Figure 3: Non-dimensional breakup length verses chamber pressure for injection velocities of 5,10 15 and 20 m/s. d_o=1.194 mm, L/D=18.4, θ=60°. Error bars represent standard deviations from the 30 images.

Impact waves were originally proposed by Dombrowski and Hooper [9], who observed the formation of disturbances very close to the point of impingement. Impact waves have been described as disturbances in the jets at the point of impact either due to turbulent fluctuations in the pre-impinging jets or due to a disturbance generated by the jet impact, such as an oscillating stagnation point [10]. When the inertial forces due to momentum fluctuations at the point of impact exceed the surface tension forces maintaining the sheet integrity, breakup could occur.

At atmospheric back-pressure, cavitation was found to occur for jet velocities greater than 17 m/s. At chamber pressures higher than 0.25 MPa cavitation did not occur for any jet velocity below 22 m/s. While cavitation has been known to affect breakup length for short L/D single orifice injectors [11], no distinct change in breakup length is observed here when crossing between cavitating and non-cavitating regimes.

Chamber pressure is observed to both decrease the breakup length and render breakup length insensitive to injection velocity (Fig. 3). Also note that at V_j=20 m/s breakup length is nearly independent of chamber pressure. At conditions of either high injection velocity or high chamber pressure breakup length is very short compared to typical combustion chamber lengths. This is a fortuitous condition when modeling combustion processes with impinging jet sprays as the injectors are usually treated as sources of droplets emanating from the impingement point. [6].

Anderson *et al.* [5] measured sheet breakup length at chamber pressures up to 1.05 MPa and found that the breakup length could be correlated with Weber number based on the liquid jet properties and gas-to-liquid density ratio. Figure 4 is a plot of non-dimensional breakup length measured in this study as a function of $We_j(\rho_g/\rho_l)^2$ along with the correlation of Anderson *et al.* Also shown in Figure 4 is a correlation derived here showing a greater gas density dependence over the extended range of gas densities studied here. The shorter breakup lengths measured here might indicate a Reynolds number dependency since the orifice diameter used here was about twice as large as that used by Anderson. Note however that this correlation is only a rough approximation and does not capture the true effect of injection velocity over the entire range of pressures studied. The R^2 value for this correlation is 0.79. R^2 is the square of the correlation coefficient and a measure of the degree of fit. A perfect correlation would have a R^2 value of 1.0

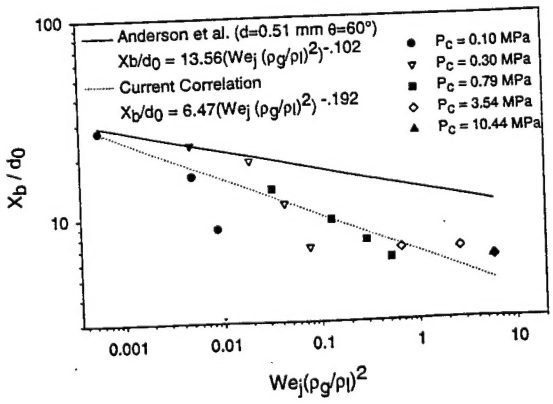

Figure 4: Non-dimensional breakup length as a function of the correlating parameter along with the correlation of Anderson *et al.* [5]. d_o=1.194 mm, L/D=18.4, θ=60°.

parameter n at an axial distance of 46 mm is plotted in Figure 8.

$$\frac{dF(D)}{dD} = nbD^{n-1}\exp\left[-bD^{n}\right] \quad (5)$$

The width of the distribution is seen to initially decrease with increasing chamber pressure but then begins to increase as chamber pressure is increased beyond 3 MPa. The decrease in $1/n$ at the lower chamber pressures is consistent with the findings of Lourme [2]. The decrease in the width of the distribution could be due to breakup of the larger droplets into smaller droplets which are already present in very large number densities, which was evident from Fig. 7. The elimination of the tail of the distribution would result in an overall decrease in the width of the distribution. The sudden increase in the width of the distribution for chamber pressures greater than 3 MPa is not clearly understood. Also note that the width of the distribution increases with increasing injection velocity which would be expected with increasing atomization energy.

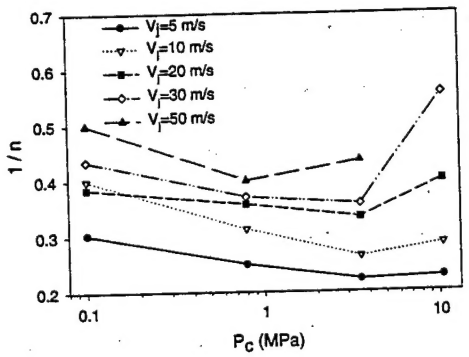

Figure 8. Inverse of Rosin-Rammler parameter, n verses chamber pressure for several injection velocities. d_o=1.194 mm, L/D=18.4, θ=60°, x=46 mm.

The effect of axial distance on the droplet size distribution was found to be even more complex than the effect on mean droplet size, therefore a correlation of n with injector operating conditions was made only for the axial location of 46 mm (Eqn. 6). The axial distance of 46 mm was chosen because this is the measurement point closest to the impingement point and thus the most useful as a modeling boundary condition.

$$n = 3.38\rho_g^{0.22}V_j^{-0.10\rho_g^{0.30}} \quad (6)$$

The R^2 correlation coefficient for Equation 6 was 0.94. The Rosin-Rammler parameter, b, can be related to D_{32} through the relationship;

$$b = \left[\frac{1}{nD_{32}\Gamma\left(1-\frac{1}{n}\right)}\right]^2 \quad (7)$$

where Γ can be obtained from gamma function tables.

Summary and Conclusions

Measurements of liquid sheet breakup length, mean droplet size and size distribution for jet velocities up to 50 m/s and chamber pressures up to 10.44 MPa have been presented. Breakup length was compared to calculations based on linear stability theory. General conclusions are as follows:

- Breakup length decreases with both increasing injection velocity and chamber gas density. The decrease in breakup length is attributed to an increase in impact wave instability and/or an increase in aerodynamic stresses on the liquid sheet at the higher injection velocities and chamber pressures.

- At either high injection velocity or high gas density the breakup length is very small and nearly independent of the injector operating conditions.

- Linear stability theory greatly over-predicts the breakup length at low gas densities where aerodynamic stresses are small and impact wave breakup would predominate. At higher chamber pressures, agreement between experiment and theory improves as aerodynamic stresses increase relative to impact wave instabilities which would be less sensitive to gas density.

- Mean droplet size is mildly dependent on chamber pressures for P_c less than about 3 MPa. At higher pressures, mean droplet size decreases significantly with increasing pressure and distance from the impingement point. Secondary atomization is believed to be the dominant mechanism behind pressure effects on droplet size and is evidenced through a decrease in number density of the larger droplet sizes at the highest chamber pressure.

- The width of the droplet size distribution initially decreased with increasing gas density as the largest droplets are removed from the distribution by secondary atomization. Increasing the chamber